

SEGMENTATION OF NEURONS BASED ON ONE-CLASS CLASSIFICATION

Paul Hernandez-Herrera¹, Manos Papadakis^{1,2} and Ioannis A. Kakadiaris¹

¹Computational Biomedicine Lab, Dept. of Computer Science
University of Houston, Houston, TX

²Department of Mathematics, University of Houston, Houston, TX

ABSTRACT

In this paper, we propose a novel one-class classification method to segment neurons. First, a new criterion to select a training set consisting of background voxels is proposed. Then, a discriminant function is learned from the training set that allows determining how similar an unlabeled voxel is to the voxels in the background class. Finally, foreground voxels are assigned as those unlabeled voxels that are not classified as background. Our method was qualitatively and quantitatively evaluated on several dataset to demonstrate its ability to accurately and robustly segment neurons.

1. INTRODUCTION

Neurons are the main part of the nervous system. They allow processing and transmission of information. Thus, in order to understand the neuronal process at the cellular level, it is necessary to develop mathematical models allowing simulation of the neuronal function. The first step of this process is the segmentation of the neuron from the background in imaging data. Manual segmentation requires an excessive amount of effort due to the large amount of data and is likely to suffer from human errors. Therefore, it is necessary to develop automatic methods for the segmentation of neurons. The main challenges to address when developing a neuron segmentation algorithm are: (i) irregular cross sections (i.e., not semi-elliptical cross sections such as those of vessels) of dendrites due to structures attached to the dendrites (spines); (ii) variability in the size of the dendrites to be segmented; (iii) the radius of thin dendrites can be as small as one voxel (depending on the voxel size); (iv) thin dendrites usually have low contrast; (v) contrast variation across different dataset due to different acquisition modalities; and (vi) noise.

Many approaches have been proposed to solve this segmentation problem including machine learning algorithms. Santamaria *et al.* [1] used the eigenvalues of the Hessian matrix as features to train a support vector machine (SVM) classifier where positive samples correspond to dendrites while background corresponds to negative samples. Gonzalez *et al.* [2] used 3D steerable filters to create feature vectors to train an SVM classifier. Recently, Jimenez *et al.* [3] proposed to

use isotropic low pass, high pass and Laplacian filters to compute a set of features which are trained with an SVM classifier to segment neurons. The main limitation of these approaches is the assumption that the training and testing samples follow the same distribution, which may not be true due to the large variety in dataset (there are three different imaging technologies and preparations with various resolutions and labeling methods [4]). Hence, these methods require re-training when the assumptions are not satisfied. Furthermore, due to the variability in the size of the dendrites, these approaches usually have difficulties in segmenting thin dendrites. For a complete review of neuron segmentation algorithms see [5, 6].

We propose a one-class classification method for the segmentation of dendrites and axons. First, a Laplacian filter is used to detect a training set consisting of voxels belonging to the background. These voxels are used to train a discriminant function which allows determining how similar an unlabeled voxel is to the voxels in the background class. Finally, the voxels that are rejected as background are labeled as foreground. Our contributions are: (i) a novel one-class classification approach to segment the background. To the best of our knowledge, this is the first attempt to segment the neuron by using one-class classification in confocal, multiphoton, and bright-field microscopy images; (ii) a novel criterion to easily select a training set of background voxels by using an isotropic Laplacian filter. Laplacian filters are mostly used for edge or interface surface detection. We demonstrate with our results that background detection is more accurate in this type of image. (iii) a novel implicit discriminant function that allows the enhancement of the background using a single scale. Previous approaches [7] used the feature vector to create explicit functions which were analyzed at multiple scales to enhance tubular structures.

The remainder of the paper is organized as follows: in Sec. 2 we describe the method for neuron segmentation, Sec. 3 presents results in real dataset, and we present our conclusions in Sec. 4.

2. METHODS

Algorithm 1 describes the proposed method One-Class Classification for SEgmentation of Neurons (OCCSEN). In this

section, each step of our approach is explained in detail.

Algorithm 1 OCCSEN

Input: A 3D image stack I and a radius σ

Output: Label 0 for background and 1 for neurons

Step 1: Select a training set of background voxels

Step 2: Extract local shape information (features)

Step 3: Estimate discriminant function

Step 4: Segment neurons

Step 5: Post-process the segmentation result

Step 1: The Laplacian operator has been widely used to extract edges by detecting zero crossings. In this paper, the isotropic windowed Laplacian operator is used to identify voxels belonging to the background of the 3D image stack I . First, the Laplacian filter is constructed in the frequency domain as:

$$\widehat{F}_{n,k}^L(\xi) = -\|\xi\|^2 \widehat{F}_L(c_{n,k}^2 \|\xi\|^2), \quad (1)$$

where $\widehat{F}_L(x) = P_n(x) \exp^{-x}$, $x > 0$ is a low pass filter (Ozcan *et al.* [8]), $P_n(x) = \sum_{i=0}^n x^i / i!$ is the n^{th} order Taylor polynomial for the exponential function and $c_{n,k} = \sqrt{2n+1} / (\sqrt{2k\pi})$ is a constant that controls the transition band and the cut-off frequency of the filter. The parameters n and k play an important role in the design of the filter; n controls the transition band with large values corresponding to small transitions and k determines the cut-off frequency. Thus, the Laplacian $L_{n,k}^I$ of the 3D image stack I is given by:

$$L_{n,k}^I = \mathcal{F}^{-1} \{ \widehat{F}_{n,k}^L(\xi) \cdot \widehat{I}(\xi) \}, \quad (2)$$

where \mathcal{F}^{-1} is the inverse Fourier transform and \widehat{I} is the Fourier transform of the 3D image stack I .

We assume that a cross section profile of a dendrite normal to the orientation of the centerline reaches its maximum intensity value in the center of the dendrite and the intensity decreases from the center to the boundary. Note that a typical 3D image stack of a neuron usually satisfies these assumptions. Then, the Laplacian of the 3D image stack (Eq. (2)) has the following properties (Ozcan *et al.* [8]): (i) its values are close to zero at the boundary of the neuron; (ii) it is negative inside the neuron; (iii) it is positive near the exterior of the neuron; and (iv) it produces oscillations between positive and negative values on the exterior of the neuron. From properties (ii) and (iv), any voxel with positive response to the Laplacian operator belongs to the exterior of the neuron. In addition, from properties (i) and (iii), there are positive values close to the boundary of the neuron which is important to have a representative training set of background voxels. From the previous observations, a training set B of background voxels is selected by using two different scales k_1 and k_2 for the Laplacian filter:

$$B = \{v \mid (L_{n,k_1}^I(v) > 0) \vee (L_{n,k_2}^I(v) > 0)\}, \quad (3)$$

where v is a voxel in I . The frequency content of thick dendrites predominantly resides in low frequencies while thin dendrites occupy more high frequencies. Hence, we customize the filters to suit the anticipated sizes of dendrites by adjusting their cut-off frequency: by selecting a small factor $k \in (0, 0.2)$, we focus only on low frequencies and thus capture thick dendrites. Increasing the value of k allows detection of thinner structures. Note that two scales are used to accurately detect thin and thick neurons. Selecting the appropriate value for k is important to obtain a good training set of background voxels.

Step 2: Local shape information from the 3D image stack is captured by using the eigenvalues ($|\lambda_1| \leq |\lambda_2| \leq |\lambda_3|$) of the Hessian matrix $H_{ij}^\sigma(v) = \frac{\partial^2 (I * G_\sigma)}{\partial v_i \partial v_j}(v)$ where G_σ is a Gaussian filter at scale σ . Frangi *et al.* [7] demonstrated that the eigenvalues of the Hessian matrix are good features to enhance tubular structures (TS) from other structures. For example, if $|\lambda_1| \approx 0$, $|\lambda_1| \ll |\lambda_2|$ and $\lambda_2 \approx \lambda_3$, indicate an ideal TS; if $\lambda_1 \approx \lambda_2 \approx \lambda_3 \approx 0$, a noisy structure is present. Frangi *et al.* also demonstrated that the parameter σ is well suited to detect a TS with radius σ . Specifically, a small scale σ can detect thin TS while large scales are more suitable for thick TS. Note that there is a correlation between the parameters σ of the Gaussian filter and k of the Laplacian filter for detecting structures of the same size.

Step 3: By learning the different configurations of eigenvalues, explicit cost functions can be constructed to enhance TS. Those discriminant functions use the property that for an ideal tubular structure λ_1 is low and λ_2, λ_3 have large negative values [7]. In this work, we propose to indirectly segment dendrites by creating a discriminant function from the empirical distribution of the training set B of background voxels which assigns values close to one for voxels in the background and values close to zero in the foreground. A three step approach is used to generate the discriminant function: (i) compute the empirical distribution of the eigenvalues corresponding to the training set B ; (ii) transform the distribution using a monotonic function to create a discriminant function; and (iii) smooth the discriminant function.

Estimate background distribution: The distribution of the two eigenvalues¹ $\lambda_2(v)$ and $\lambda_3(v)$ from the training set B provides information on which points should be assigned with high probability to belong to background. The higher the value of the distribution, the more likely the point belongs to the background. Note that there are enough sample points to accurately approximate the background distribution since the number of points in the detected training set B is at least 50% of the points in the 3D image stack I . The distribution of the eigenvalues $\lambda_2(v)$ and $\lambda_3(v)$ of voxels in B is approximated (Eq. (3)) using a 2D histogram. The histogram is

¹We use only the two largest eigenvalues since they provide enough shape information and we avoid the additional computational effort to compute the 3D distribution.

computed as:

$$P(i, j) = c([b_{1,i}, b_{1,i+1}) \times [b_{2,j}, b_{2,j+1})), \quad (4)$$

where $c(R)$ represents the number of feature vectors that belong to the two-dimensional interval R , $b_{s,k} = m_s + k \frac{M_s - m_s}{N}$, N is number of bins for the histogram, and m_s, M_s are the minimum and maximum values of the s -feature, respectively.

Transform the background distribution: From the empirical distribution P of the eigenvalues of the training set, a discriminant function C is created with values in $[0,1)$ by applying the transformation

$$C(i, j) = \frac{1 - \exp^{-P(i,j)}}{1 + \exp^{-P(i,j)}}. \quad (5)$$

This transformation assigns values close to one to any bin with $P(i, j) \geq 6$ while value zero to bins with $P(i, j) = 0$.

Smoothing the discriminant function: A disadvantage of histograms is that they result in piecewise constant functions. Hence, C is such a function. Those discontinuities are smoothed by convolving C with a Gaussian kernel $C_s = C * G_{\sigma_s}$.

Step 4: The following function is used to enhance the background:

$$E_B(v) = \begin{cases} 1 & \text{if } v \in B \\ C_s(Q(\lambda_2(v), \lambda_3(v))) & \text{otherwise} \end{cases}, \quad (6)$$

where $Q(\lambda_2(v), \lambda_3(v))$ indicates the bin position of $(\lambda_2(v), \lambda_3(v))$. Note that the discriminant function C_s is applied only to the voxels that were not selected in the training set B (Eq. (3)). The background is segmented by applying a threshold as:

$$S_B(v) = \begin{cases} 1 & \text{if } E_B(v) > T \\ 0 & \text{otherwise} \end{cases}, \quad (7)$$

which the user can vary to optimize results. The threshold T is automatically selected by computing the value C_s for each voxel in the training set B and selecting the T that correctly classifies 99% of the training set as background. Finally, dendrites are detected as those voxels that are rejected as background ($S_D = \neg S_B$).

Step 5: The segmentation S_D may still identify false dendrites which usually have few voxels. They are detected by identifying connected components using a 26-connected neighborhood and disregarding components with less than c_m voxels.

3. RESULTS

We qualitatively and quantitatively evaluated the performance of the proposed approach on numerous dataset. The DIA-DEM dataset [4] was used to evaluate our algorithm since it is a representative sample of data. We report results for three out

of six dataset (Neocortical Layer 1 Axons (NL), Neuromuscular Projection Fibers (NP) and Olfactory Projection Fibers (OP)) due to space limitations.

Parameter Settings: There are seven parameters ($n, c_m, N, \sigma_s, k_1, k_2,$ and σ). We choose $n = 60$ because it provides a small transition band, $c_m = (4 * \sigma)^3$ to remove connected components with few voxels, the parameter N depends on the size of the training set B : the larger the training set, the smaller the bin size to obtain a good approximation of the distribution. Hence, we randomly select 1M samples from B and fix $N = 500$, we set $\sigma_s = 5$ because it is an adequate value for the size of the histogram, $k_2 = 1.5k_1$ because it allows detection of thicker dendrites and we have experimentally estimated the relationship $k_1 \approx 0.5913\sigma^{-1}$ used to detect structures of the same size between σ and k_1 . Thus, all the parameters are fixed except σ . The user has to select the parameter σ to perform segmentation. The parameter σ allows selection of the sensitivity to the radius to detect. Thus, if we want to detect dendrites with r voxels radius, we should select a σ in the range $[r - \epsilon, r + \epsilon]$ where ϵ is a small value.

We compare our method with the segmentation method of Jimenez *et al.* [3] by comparing the extracted centerline. The parameter settings for the segmentation method of Jimenez *et al.* were optimized for each dataset to obtain the best segmentation. Their centerline extraction method depends heavily on the accuracy of the segmentation. To quantitatively measure the performance of our method, we use the metrics used in [3], namely Recall = $S_C / (S_C + S_m)$ and Miss-Extra-Score (MES) = $(S_G - S_m) / (S_G + S_e)$, where S_C is the total length of the correct segments by each algorithm, S_G is the total length of the manual reconstruction. The symbols S_m and S_e denote the total length of missing and extra segments in the automatically traced centerline, respectively. The dendrites from the OP dataset have small radii between 1 and 4 voxels and those from the NM dataset have high radii between 3 and 10 voxels. Hence, we use small $\sigma \in \{1.00, 1.25, 1.50, 1.75\}$ for OP segmentation and large $\sigma \in \{3.0, 4.0, 5.0\}$ for NM segmentation. The σ resulting in the best segmentation results was used for comparison. Tables 1 and 2 summarize the performance results for OP and NP dataset. Our segmentation results improve the average Recall and MES, indicating that our method provides a more accurate segmentation of the dendrites than method A. Figure 1 depicts qualitative results in a 3D image stack from the NL dataset. Figure 1(a) depicts a volume rendering of the 3D image stack. Note that there is very low contrast for thin dendrites. Figures 1(b,c) depict the segmentation for Jimenez *et al.* and our approach ($\sigma = 2$), respectively. Note that our approach can capture the low contrast dendrites while Jimenez *et al.* fails to segment them.

4. CONCLUSION

In this paper, we presented a novel one-class classification method to segment neurons. Our qualitative and quantita-

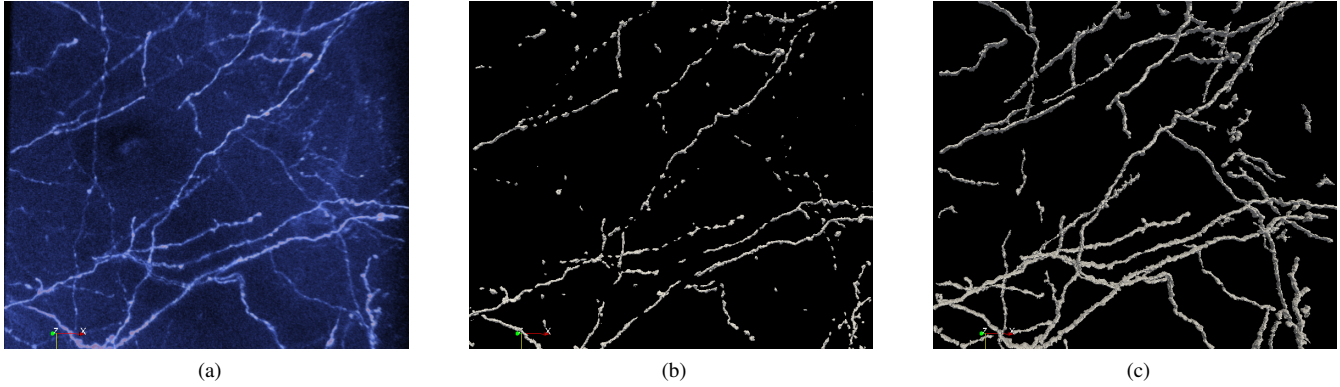


Fig. 1. (a) Volume rendering of a 3D stack from NL dataset; (b) segmentation of Jimenez *et al.* [3]; and (c) our segmentation.

Table 1. Performance evaluation on the OP dataset (A: Jimenez *et al.* [3], B: OCCSEN.)

Stack\method	Recall		MES	
	A	B	A	B
1	0.94	0.96	0.93	0.94
3	0.74	0.92	0.74	0.88
4	0.88	0.91	0.83	0.81
5	0.74	0.84	0.71	0.78
6	0.95	0.98	0.94	0.96
7	0.94	0.95	0.94	0.94
8	0.98	0.99	0.97	0.97
9	0.82	0.91	0.78	0.81
Average	0.87	0.93	0.85	0.89

Table 2. Performance evaluation on 30 volumes from the NP dataset (A: Jimenez *et al.* [3], B: OCCSEN.)

Stack\method	Recall		MES	
	A	B	A	B
Average	0.94	0.97	0.93	0.95

tive results shows that our method can effectively segment dendrites. The main advantages of our approach are: (i) it works for a wide range of acquisition modalities; (ii) it can accurately segment thick or thin dendrites; (iii) it requires minimal user intervention; and (iv) the user can easily select the correct value of σ if the likely size of dendrite is known.

Acknowledgments: This work was supported in part by: NSF DMS 0915242, NHARP 003652-0136-2009, CONACYT and the UH Hugh Roy and Lillie Cranz Cullen Endowment Fund.

5. REFERENCES

- [1] A. Santamaria-Pang, C.M. Colbert, P. Saggau, and I.A. Kakadiaris, “Automatic centerline extraction of irregular tubular structures using probability volumes from multiphoton imaging,” in *Proc. Medical Image Computing and Computer-Assisted Intervention*, Brisbane, Australia, Oct. 29 - Nov. 2 2007, pp. 486–494.
- [2] G. Gonzalez, F. Aguet, F. Fleuret, M. Unser, and P. Fua, “Steerable features for statistical 3D dendrite detection,” in *Proc. International Conference on Medical Image Computing and Computer-Assisted Intervention*, London, UK, 20-24 Sep 2009, vol. 5762, pp. 625–32.
- [3] D. Jimenez, M. Papadakis, D. Labate, and I.A. Kakadiaris, “Improved automatic centerline tracing for dendritic structures,” in *Proc. International Symposium on Biomedical Imaging: From Nano to Macro*, San Francisco, CA, April 8-11 2013, pp. 1050–1053.
- [4] K.M. Brown, G. Barrionuevo, A.J. Canty, V.D. Paola, J.A. Hirsch, G. Jefferis, J. Lu, M. Snippe, I. Sugihara, and G.A. Ascoli, “The DIADEM data sets: representative light microscopy images of neuronal morphology to advance automation of digital reconstructions,” *Neuroinformatics*, vol. 9, no. 2-3, pp. 143–157, 2011.
- [5] E. Meijering, “Neuron tracing in perspective,” *Cytometry Part A*, vol. 77A, no. 7, pp. 693–704, 2010.
- [6] D.E. Donohue and G.A. Ascoli, “Automated Reconstruction of Neuronal Morphology: An Overview,” *Brain Research Reviews*, vol. 67, pp. 94–102, 2011.
- [7] A.F. Frangi, W.J. Niessen, K.L. Vincken, and M.A. Viergever, “Multiscale vessel enhancement filtering,” in *Proc. Medical Image Computing and Computer Assisted Intervention*, Cambridge, MA, Oct. 11-13 1998, vol. 1496, pp. 130–137.
- [8] B. Ozcan, D. Labate, D. Jiménez, and M. Papadakis, “Directional and non-directional representations for the characterization of neuronal morphology,” in *Proc. Wavelets and Sparsity XV*, M. Papadakis D. Van De Ville, V. Goyal, Ed., San Diego, CA, August 25-29 2013, SPIE, vol. 8858.